Cellular Physiology and Biochemistry

Cell Physiol Biochem 2018;46:160-177
DOI: 10.1159/000488419
Published online: March 26, 2018
Accepted: February 13, 2018

Original Paper

Inhibition of Cgkii Suppresses Seizure Activity and Hippocampal Excitation by Regulating the Postsynaptic Delivery of Glua1

Juan Gu[a,b] Xin Tian[a] Wei Wang[a] Qin Yang[a] Peijia Lin[a] Yuanlin Ma[a] Yan Xiong[a] Demei Xu[a] Yanke Zhang[a] Yong Yang[a] Shanshan Lu[a] Zijun Lin[a] Jing Luo[a] Fei Xiao[a] Xuefeng Wang[a,c]

[a]Department of Neurology, the First Affiliated Hospital of Chongqing Medical University, Chongqing Key Laboratory of Neurology, Chongqing, [b]Department of Neurology, Hospital (T.C.M) Affiliated to Southwest Medical University, Luzhou, [c]Center of Epilepsy, Beijing Institute for Brain Disorders, Beijing, China

Key Words
4-aminopyridine • CGKII • Epilepsy • GluA1 • Pilocarpine

Abstract
Background/Aims: The imbalance between excitation and inhibition is a defining feature of epilepsy. GluA1 is an AMPA receptor subunit that can strengthen excitatory synaptic transmission when upregulated in the postsynaptic membrane, which has been implicated in the pathogenesis of epilepsy. cGKII, a cGMP-dependent protein kinase, regulates the GluA1 levels at the plasma membrane. ***Methods:*** To explore the role of cGKII in epilepsy, we investigated the expression of cGKII in patients with temporal lobe epilepsy (TLE) and in a pilocarpine-induced rat model and then performed behavioral, histological, and electrophysiological analyses by applying either a cGKII agonist or inhibitor in the hippocampus of the animal model. ***Results:*** cGKII expression was upregulated in the epileptogenic brain tissues of both humans and rats. Pharmacological activation or inhibition of cGKII induced changes in epileptic behaviors *in vivo* and epileptic discharges *in vitro*. Further studies indicated that cGKII activation disrupted the balance of excitation and inhibition due to strengthened AMPAR-mediated excitatory synaptic transmission. Moreover, cGKII regulated epileptic seizures by phosphorylating GluA1 at Ser845 to modulate the expression and function of GluA1 in the postsynaptic membrane. ***Conclusion:*** These results suggest that cGKII plays a key role in seizure activity and could be a potential therapeutic target for epilepsy.

J. Gu, X. Tian and W. Wang contributed equally to this work.

Xuefeng Wang
and Fei Xiao

Department of Neurology, the First Affiliated Hospital of Chongqing Medical University, Chongqing Key Laboratory of Neurology, 1Youyi Road, Chongqing, 400016 (China)
E-Mail xfyp@163.com, xiaofei@hospital.cqmu.edu.cn

Introduction

Epilepsy is a common brain disorder characterized by recurrent seizures that affects more than 68 million people worldwide [1]. Although dozens of antiepileptic drugs have been developed for clinical use, nearly one-third of epileptic patients still suffer from intractable seizures [2]. Unfortunately, drug treatment efficacy and the incidence of drug-resistant epilepsy have not significantly changed in recent decades. Significant progress in antiepileptic treatments has not been achieved, suggesting that the identification of novel therapeutic targets is important for changing the current efficacy of these treatments.

TLE is the most common form of drug-resistant epilepsy. This disease is devastating due to its resultant progressive brain damage, associated behavioral disorders, and increased mortality risk [3, 4]. An imbalance between excitation and inhibition in neuronal networks is a defining feature of TLE [5]. AMPA receptors (AMPARs) are hetero-tetrameric cation channels that mediate the majority of fast excitatory synaptic transmissions [6]. Subunits GluA1 to GluA4 form functionally different tetramers. AMPARs containing GluA2 are impermeable to calcium, whereas AMPARs are permeable to calcium when GluA2 is absent [7]. In most areas of the brain, AMPARs are GluA1/GluA2 heteromers [8]. Increased expression of the GluA1 subunit at the postsynaptic membrane could strengthen AMPAR-mediated synaptic transmission [9, 10], resulting in an imbalance between excitation and inhibition of the neural network, which might lead to further neuronal hyperexcitability. An extensive body of evidence suggests that GluA1 is critical to the generation and development of epileptic seizures [6, 11, 12].

cGMP-dependent protein kinases (cGKs) are serine/threonine kinases. Two types of cGK proteins, cGKI and cGKII, are present in mammalian tissues, and cGKI has two isozymes, cGKIα and cGKIβ [13]. Experiments conducted by el-Husseini et al. [14] have demonstrated that cGKI is enriched primarily in the cerebellum, whereas cGKII is expressed widely throughout the brain. cGKII is involved in brain disorders such as anxiety-like behaviors and spatial memory deficits [15, 16]. In addition, recent studies have demonstrated that cGKII phosphorylates GluA1 at serine 845 (S845), resulting in GluA1 augmentation at the cell membrane [17, 18]. The GluA1 subunit is functionally important in epilepsy, and the link between GluA1 and cGKII led us to hypothesize that cGKII dysfunction is involved in epilepsy.

In the present study, we investigated the role of cGKII in epileptic seizures, the influence of cGKII on neuronal excitability, and the possible associated underlying mechanisms. First, we tested whether cGKII expression was altered in epileptic patients and in pilocarpine-induced epileptic rats and found that cGKII expression was upregulated in the brain tissues of both patients and rat models. We subsequently studied the effects of cGKII on seizure activities and found that cGKII disruption induced changes in epileptic behaviors *in vivo* and epileptic discharges *in vitro*. Electrophysiological recordings were then obtained to explore whether cGKII dysfunction changed excitatory synaptic transmission and the underlying mechanisms during epileptic stimulation. Our findings suggested that cGKII could regulate epilepsy by modulating neuronal AMPAR activity and might be a new target for novel anticonvulsant drugs.

Materials and Methods

Study approval

All the animal procedures in this study were approved by the Institutional Animal Care and Use Committee of Chongqing Medical University. The research on human brain tissue was performed in accordance with the ethical requirements of the Declaration of Helsinki of the World Medical Association and was approved by the ethics committee for human research of Chongqing Medical University. All patients or their families signed an informed consent form.

Human subjects

Sixteen epileptic and 10 control brain tissue samples were randomly selected from the epilepsy and control brain tissue banks established by our research team, respectively [19]. The samples in our epilepsy brain tissue bank were all obtained from drug-refractory epileptic patients. The patient diagnosis complied with the criteria established by the International League Against Epilepsy (ILAE) [2]. Table 1 summarizes the clinical features of the 16 epileptic patients. The specimens in our control tissue bank originated from patients who underwent surgery to treat increased intracranial pressure caused by head trauma, and Table 2 summarizes the clinical characteristics of the 10 control patients. The brain tissue inclusion criteria and processing protocol are described in our previous publications [19, 20]. No significant difference in age or the female/male ratio was observed between the TLE group and the control group (P>0.05).

Table 1. Clinical features of the TLE patients. AEDs, antiepileptic drugs; EP, epileptic patient; M, male; F, female; CBZ, carbamazepine; CZP, clonazepam; PB, phenobarbital; PHT, phenytoin; TPM, topiramate; VPA, valproate; OXC, oxcarbazepine; LTG, lamotrigine; TN, temporal neocortex; L, left; R, right; NL, neuronal loss; G, gliosis

Subject	Age (year)	Gender (M/F)	Course (year)	AEDs before surgery	Resection tissue	Pathology
EP 1	22	F	12	CBZ, PHT, VPA	TN, L	NL, G
EP 2	31	F	15	CBZ, PB, PHT	TN, L	NL, G
EP 3	27	M	18	CBZ, PB, PHT, VPA	TN, R	NL, G
EP 4	18	F	7	CBZ, TPM, VPA	TN, L	NL, G
EP 5	15	M	9	CBZ, CZP, VPA	TN, L	NL, G
EP 6	25	M	17	CBZ, PB, PHT, VPA	TN, L	NL, G
EP 7	36	F	24	CBZ, CZP, PB, PHT, VPA	TN, L	NL, G
EP 8	29	F	11	OXC, TPM, VPA	TN, R	NL, G
EP 9	17	F	6	CBZ, LTG, PB	TN, L	NL, G
EP 10	10	M	7	CBZ, TPM, VPA	TN, R	NL, G
EP 11	24	M	13	CBZ, PB, TPM, VPA	TN, R	NL, G
EP 12	22	F	12	CBZ, PHT, TPM, VPA	TN, R	NL, G
EP 13	33	F	21	OXC, PB, PHT	TN, L	NL, G
EP 14	23	M	15	CBZ, LTG, TPM, VPA	TN, L	NL, G
EP 15	38	F	19	CBZ, PHT, TPM, VPA	TN, R	NL, G
EP 16	19	M	10	PHT, TPM, VPA	TN, R	NL, G

Table 2. Clinical features of the control patients. C, control; M, male; F, female; TN, temporal neocortex; L, left; R, right; N, normal

Subject	Age (year)	Gender (M/F)	Clinical diagnosis	Resection tissue	Pathology
C1	15	M	Trauma	TN, R	N
C2	18	M	Trauma	TN, R	N
C3	27	F	Trauma	TN, L	N
C4	35	M	Trauma	TN, L	N
C5	24	M	Trauma	TN, R	N
C6	22	M	Trauma	TN, L	N
C7	31	F	Trauma	TN, R	N
C8	41	F	Trauma	TN, R	N
C9	33	M	Trauma	TN, R	N
C10	21	F	Trauma	TN, L	N

Experimental rats

Healthy adult male Sprague-Dawley rats (weighing approximately 220 g) were purchased and housed at the Experimental Animal Center of Chongqing Medical University. Three rats per cage were reared under a normal circadian rhythm at a controlled temperature (23 ± 1°C) and had free access to food and water.

The rat pilocarpine-induced seizure model was prepared as reported earlier [21]. SD rats were randomly selected. First, lithium chloride (127 mg/kg) was injected intraperitoneally, and after approximately 18–20 hours, atropine (0.2 ml/100 g) was administered intraperitoneally. The rats were then treated with pilocarpine (50 mg/kg) intraperitoneally after 30 minutes. Finally, the seizure severity was scored by closely observing the behavioral changes in rats according to the Racine scale as follows [22]: stage 0, no seizures; stage 1, rigid posture with facial twitching; stage 2, rhythmic head nodding; stage 3, unilateral forelimb clonus; stage 4, bilateral forelimb clonus with standing; and stage 5, seizures with loss of balance and falling. Recurrent stage 4 to 5 seizures were defined as SE. Rats in which SE was successfully induced were administered atropine (0.2 ml/100 g) and diazepam (10 mg/kg) intraperitoneally 60 minutes after seizure onset to terminate the seizures. Rats that failed to exhibit SE were included in the control group. Subsequent behavior changes were observed by video monitors for at least two months. Rats with SRSs were included in the experimental group, and other rats that experienced SE but not SRSs were included in another control group.

Surgical procedures and EEG recordings

Healthy adult male SD rats (n = 24) were randomly selected and anesthetized by intraperitoneal administration of 3.5% chloral hydrate (1 ml/100 g). The Brain Atlas by Paxinos et al [23].was used to

position the lateral ventricles (anterior/posterior, -1.5; medial/lateral, 1.0; and dorsal/ventral, -3.5). A microinjection catheter was implanted into the left lateral ventricle and fixed with dental cement onto the skull. For EEG recording, a microwire array (2 × 4 array of platinum-iridium alloy wire, 25 μm in diameter, Plexon, Dallas, TX, USA) was implanted into the right dorsal hippocampus (anterior/posterior, -4.0; medial/lateral, 2.6; and dorsal/ventral, -2.8). The subsequent experiments were conducted after at least one week to allow the rats to recover from surgery. 8-Br-cGMP (500 μM, 5 μL, Sigma, St. Louis, MO, USA), KT5823 (2 μM, 5 μL, Sigma, St. Louis, MO, USA), ACSF (5 μL, see slice preparation), or DMSO (5 μL, diluted 1000-fold by ACSF) was slowly administered into the lateral ventricle through the microinjection catheter. Four hours later, pilocarpine was injected intraperitoneally. All the seizure activities induced by pilocarpine were recorded by two experimental researchers blinded to the treatment groups. EEGs were recorded 15 minutes before pilocarpine injection. The EEGs were recorded using the Omniplex® D neural Data Acquisition System (Plexon, Dallas, TX, USA). The EEG signals were filtered at 0.1–1000 Hz, digitized at 4 kHz, and analyzed using the Neuro Explorer v4.0 (Plexon, Dallas, TX, USA).

Tissue preparation

Both human and rat brain tissues were divided into two portions immediately after surgical removal. One portion was immediately placed in liquid nitrogen for western blot analysis. The other portion was fixed in 4% paraformaldehyde for 48 hours and then cut into 10-μm-thick sections using a freezing microtome and stored at -20°C for immunofluorescence staining.

Western blot analysis

Western blot analysis was performed according to published protocols [19]. The total protein from homogenized rat and human brain tissues was extracted in RIPA lysis buffer (Beyotime Institute of Biotechnology, Jiangsu, China) following the manufacturer's recommended protocols. The protein concentration was determined using the Enhanced BCA Protein Assay Kit (Beyotime Institute of Biotechnology, Jiangsu, China). Equal amounts of protein (50 μg) from each sample were loaded into each gel lane, separated on 8% polyacrylamide Tris-HCl gels, and electrotransferred onto Immobilon polyvinylidene difluoride (PVDF) membranes (Millipore, Billerica, MA, USA) using an electrophoretic transfer system (Bio-Rad Laboratories, USA). The PVDF membranes were then incubated in 5% skim milk/Tween-20-Tris-buffered saline for 60 minutes at 37°C. The PVDF membranes were then incubated overnight at 4°C with the following primary antibodies: rabbit polyclonal anti-cGKI (sc-25429, 1:200 dilution, Santa Cruz Biotechnology, Santa Cruz, CA, USA), rabbit polyclonal anti-cGKII (sc-25430, 1:200 dilution, Santa Cruz Biotechnology), mouse monoclonal anti-GluR1 (sc-13152, 1:200 dilution, Santa Cruz Biotechnology), rabbit monoclonal anti-phospho-GluA1-Ser^{845} (04-1073, 1:3000 dilution, Millipore), or mouse monoclonal anti-GAPDH (1:1000 dilution, Beyotime). The membranes were washed three times with Tween-20-Tris-buffered saline (TBST) and then incubated with goat anti-rabbit or goat anti-mouse peroxidase-conjugated secondary antibodies (1:2000, Beyotime) at 37°C for 1 hour. Images were acquired using a charge-coupled device camera (Bio-Rad, Hercules, CA, USA). The blot intensities were analyzed using Quantity One software (Bio-Rad, Hercules, CA, USA).

Immunofluorescence staining

The frozen sections were air dried and fixed in 4% paraformaldehyde at room temperature for 5 minutes. Antigen recovery was performed by treating the sections with sodium citrate buffer and heating them in a microwave oven for 15 minutes. The sections were blocked in 10% goat serum (Zhongshan Golden Bridge Inc., Beijing, China) at 37°C for 60 minutes and then incubated with the following mixture of primary antibodies overnight at 4°C: rabbit polyclonal anti-cGKII (1:50) either with mouse monoclonal anti-MAP2 (1:50) or mouse monoclonal anti-GFAP (1:50) or with mouse monoclonal anti-PSD95 (1:200) and guinea pig monoclonal anti-vGlut1 (1:200). The sections were washed and incubated with a mixture of DyLight 488-conjugated AffiniPure goat anti-rabbit IgG (1:100) and DyLight 549-conjugated AffiniPure goat anti-mouse IgG (1:100) or with a mixture of DyLight 488-conjugated AffiniPure goat anti-mouse IgG (1:100), DyLight 549-conjugated AffiniPure goat anti-rabbit IgG (1:100), and DyLight 633-conjugated AffiniPure goat anti-guinea pig (1:100) in the dark at 37°C for 60 minutes. The nuclei were stained with DAPI. The sections were then cover-slipped with 1:1 glycerol/PBS. The fluorescence was examined by laser scanning confocal microscopy (Leica Microsystems Heidelberg GmbH, Germany).

Slice preparation

The experiments were conducted on male Sprague-Dawley rats (16–21 days of age). The animals were anesthetized using 3.5% chloral hydrate (1 ml/100 mg) and were sacrificed by decapitation. Their brains were quickly placed into an ice-cold cutting solution containing 2.5 mM KCl, 6 mM $MgCl_2$, 1 mM $CaCl_2$, 1.25 mM NaH_2PO_4, 26 mM $NaHCO_3$, 220 mM sucrose, and 10 mM glucose. Brain slices (400-μm thick) were cut using a vibratome (Leica VT1200S) after approximately 1 minute of freezing. The slices were then incubated for at least 1 hour before recording at room temperature (24–26°C) in oxygen-saturated ACSF containing 124 mM NaCl, 3 mM KCl, 2 mM $MgCl_2$, 2 mM $CaCl_2$, 1.23 mM NaH_2PO_4, 26 mM $NaHCO_3$, and 10 mM glucose. All the solutions were continuously saturated with 95% O_2/5% CO_2.

Electrophysiology

Recordings were performed using a patch-clamp amplifier (MultiClamp 700B, Molecular Devices) in either voltage- or current-clamp mode filtered at 2 kHz and digitized at 10 kHz (DigiData 1440A and PClamp10.3, Molecular Devices). Glass microelectrodes (ITEM #:BF150-86-10, Sutter Instrument Co.) were fashioned on a vertical micropipette puller (P-97, Sutter Instrument Co.), and the resistance of the microelectrodes was in the range of 3–6 MΩ when filled with internal solution. The recordings were performed using ACSF at a recording chamber perfusion rate of 2 mL/min. The cells were visualized using infrared-differential interference contrast microscopy (Olympus, Tokyo, Japan), and the microelectrodes were positioned using a micromanipulator. After a tight seal (electrode resistance > 2 GΩ) was formed between the electrode tip and the cell surface, slight suction was briefly applied until a whole-cell patch-clamp recording configuration was achieved (access resistance < 20 MΩ). The series resistance (15–30 MΩ) was compensated automatically using a MultiClamp 700B and was monitored throughout the recording, and the data were discarded if the resistance changed by more than 20%.

For extracellular field potential recording, a bipolar tungsten stimulation electrode was positioned in the Schaffer collateral pathway and stimulated at a frequency of 0.1 Hz using constant current pulses of 0.1 ms. A recording electrode filled with ACSF was placed in the stratum pyramidale of the CA1 region for the recording of stimulus-evoked population spikes. Seizure-like activity was evoked by bath application of the powerful convulsant 4AP (20 μM, 40 μM, 100 μM, or 200 μM, Sigma, St. Louis, MO, USA) for at least 10 minutes.

Whole-cell current-clamp recordings were performed according to previously described methods [24, 25]. The pipette solution contained 135 mM K-gluconate, 5 mM KCl, 10 mM HEPES, 2 mM $MgCl_2$, 5 mM EGTA, 0.5 mM $CaCl_2$, 5 mM MgATP, and 0.3 mM NaATP (pH 7.4 adjusted with KOH). The recorded CA1 pyramidal neurons were held at -50 mV by a current injection. 4AP (20 or 200 μM) was applied to evoke seizure-like activity.

For whole-cell voltage-clamp recordings, the excitatory-specific pipette solution contained 130 mM $CsCH_3SO_3$, 10 mM HEPES, 10 mM CsCl, 4 mM NaCl, 1 mM $MgCl_2$, 1 mM EGTA, 5 mM NMG, 5 mM MgATP, 0.5 mM Na_2GTP, and 12 mM phosphocreatine (pH adjusted to 7.2 with CsOH, 275–290 mOsm). The inhibitory-specific pipette solution contained 10 mM HEPES, 100 mM CsCl, 1 mM $MgCl_2$, 1 mM EGTA, 30 mM NMG, 5 mM MgATP, 0.5 mM Na_2GTP and 12 mM phosphocreatine (pH adjusted to 7.2–7.3 with CsOH, 270–280 mOsm). For all evEPSCs, the current responses were evoked using a bipolar tungsten stimulation electrode. The distance between the stimulation electrode and the recording electrode was approximately 150 μm, and the stimulation pulse duration was 40 μs. Each current response was averaged from 10 repetitive stimuli at a frequency of 0.1 Hz.

For assessments of mEPSCs, voltage-clamp recordings were performed with CA1 pyramidal neurons at a holding potential of -70 mV in the presence of picrotoxin (100 μM) and tetrodotoxin (TTX, 1 μM). mIPSCs were recorded in a similar manner but in the presence of DNQX (10 μM), D-APV (50 μM), and TTX (1 μM).

For the AMPA/NMDA ratio experiments, picrotoxin (100 μM) was added to the bath solution. The CA1 pyramidal neurons were first voltage-clamped at -70 mV, and the peak amplitude of current responses was identified as the AMPARs-mediated response. Neurons were then voltage-clamped at +40 mV, and the amplitude of the current responses at 50 ms post-stimulus was identified as the NMDAR-mediated response.

For assessments of presynaptic glutamatergic contributions, a paired-pulse protocol was performed at a holding potential of -70 mV. The paired-pulse ratio (PPR) was defined as the amplitude of the second response to the amplitude of the first response. The PPR was measured with two stimuli at an inter-pulse interval of 50 ms in the presence of picrotoxin (100 μM).

For measurements of rectification, spermine (100 μM) was added to the pipette solution, and picrotoxin (100 μM) and D-APV (50 μM) were added to the bath solution. Neurons were held at -60, -40, -20, 0, +20, or +40 mV to generate current-voltage (I-V) curves. The RI was calculated by dividing the amplitude of the average EPSCs measured at -60 mV by that measured at +40 mV.

An inhibitory peptide (TLPRNSGAG) of GluA1 phosphorylation at Ser845 and a control peptide (NRPGGTLSA) were constructed (Pepmic Co., Ltd. Suzhou, China). All the other chemicals used in this experiment were purchased from Sigma-Aldrich (St. Louis, MO, USA). The electrophysiology recordings were analyzed using Clampfit 10.3 software (Molecular Devices).

Statistical analysis

The data in these experiments are represented as the means ± standard errors (means ± s.e.m.). Differences between two groups were analyzed using unpaired or paired Student's t-test. Differences among more than two groups were analyzed by one-way ANOVA followed by Tukey's post hoc test. Categorical variables were compared using the Pearson chi-square test. Cumulative probability plots were generated with the Kolmogorov–Smirnov test. $P < 0.05$ indicates a significant difference.

Results

cGKII was upregulated in the brain tissues of epileptic patients and rat pilocarpine-induced seizure models

Western blots were performed to investigate whether the expression levels of cGKI and cGKII were changed in epileptic humans and in a rat pilocarpine-induced seizure model. The results revealed that cGKI expression was not significantly different in the temporal neocortex of patients with TLE compared with that in the control group ($p = 0.770$); however, the cGKII levels in epileptic patients were approximately 1.7-fold higher than those in the control group (**$p < 0.01$, Fig. 1a). The rats that had not developed status epilepticus (SE) within 2 months after intraperitoneal injection of pilocarpine were included as a control group (the non-SE group). The rats with SE but without spontaneous recurrent seizures (SRSs) were also included as a control group (the non-SRS group). In contrast, the rats with both SE and SRSs were

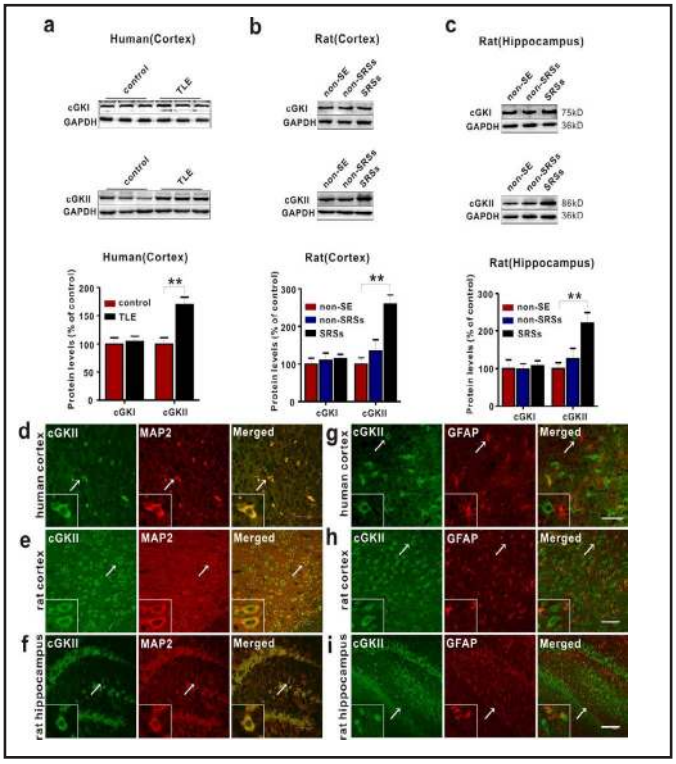

Fig. 1. cGKII expression in TLE patients and epileptic model rats. (a) cGKI and cGKII expression in the temporal neocortex tissues of non-TLE patients (control, n = 10) and TLE patients (n = 16). The expression of cGKI and cGKII was determined by western blotting. cGKI and cGKII expression in the cortex (b) and hippocampus (c) of rats in the non-SE, non-SRS, and SRS groups (n = 6). Quantification of cGKI and cGKII immunoreactivity normalized to GAPDH and to control values; GAPDH was used as a loading control. cGKII (green) is co-expressed (merged) with MAP2 (red) in the neurons (d-f) but not with GFAP (red) in the astrocytes (g-i) of TLE patients and pilocarpine seizure model rats, as demonstrated by immunofluorescent labeling. The images in the lower left corner are magnifications of the area indicated by the white arrow. Scale bar = 75 μm (Figs from the cortex), scale bar = 150 μm (Figs from the hippocampus). The significance (**$p<0.01$) was determined using Student's t-test or one-way ANOVA.

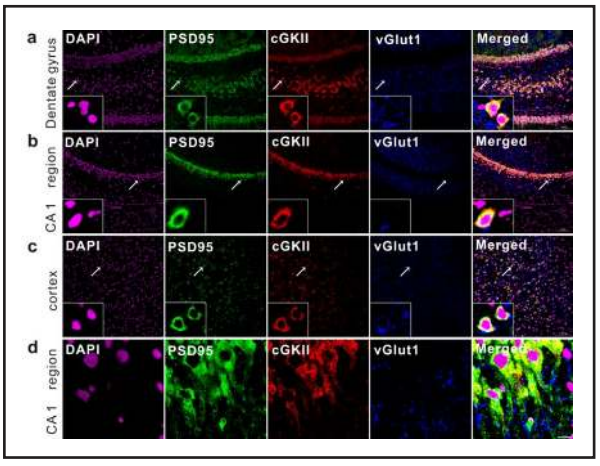

Fig. 2. cGKII accumulates in postsynaptic membranes in both the hippocampus and the cortex of rats. Vibratome sections from acute pilocarpine seizure model rats were labeled with polyclonal antibodies against PSD95 (green), vGlut1 (blue), and cGKII (red). The slices were also stained with DAPI (blue) to indicate nuclei. cGKII is co-expressed (merged) with PSD95 but not with DAPI or vGlut1 in neurons of either the hippocampus (a, b, and d) or the temporal neocortex (c). The images in the lower left corner are magnifications of the area indicated by the white arrow. Scale bar = 100 μm (Figs a, b, and c), scale bar = 10 μm (Fig. d).

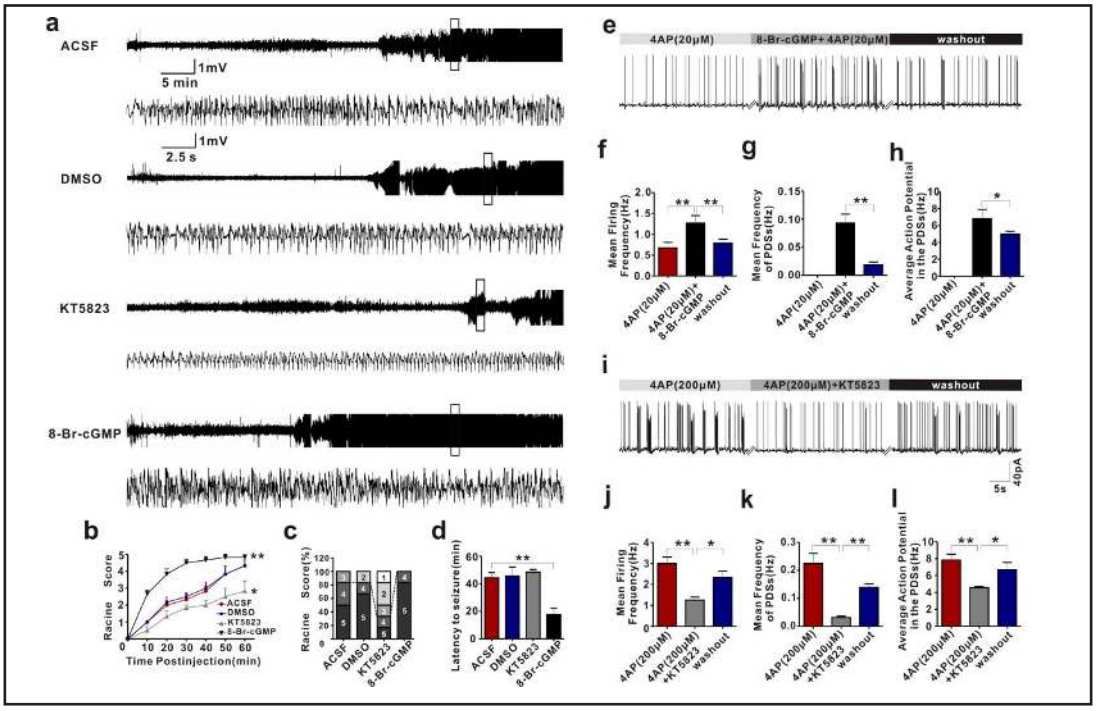

Fig. 3. Effects of the cGKII inhibitor KT5823 and agonist 8-Br-cGMP on seizure activities. SD rats were divided into four groups (n = 6 per group) and injected intracerebroventricularly with ACSF (control), DMSO, KT5823, or 8-Br-cGMP. (a) Representative traces of EEG recordings from the rats in the four groups. (b) Racine scores, (c) percentages of pilocarpine-induced generalized tonic-clonic seizures (GTCSs, seizure score of 4 or 5), (d) and onset latency in the rats. (e and i) Representative traces from the experiments performed under the whole-cell current-clamp mode. Effects of 8-Br-cGMP on the mean firing frequency (f and j), the mean frequency of PDSs (g and k), and the average action potential in the PDSs (h and l, n = 5 cells). The significance (*p<0.05, **p<0.01) was determined using one-way ANOVA or Student's t-test.

included in the experimental group (the SRS group). cGKI expression on the temporal cortex and hippocampus of the rat brain did not show significant differences among the non-SE, non-SRSs, and SRSs groups. However, cGKII expression was significantly higher in the SRS group than in the two control groups (**p < 0.01, Figs. 1b and c).

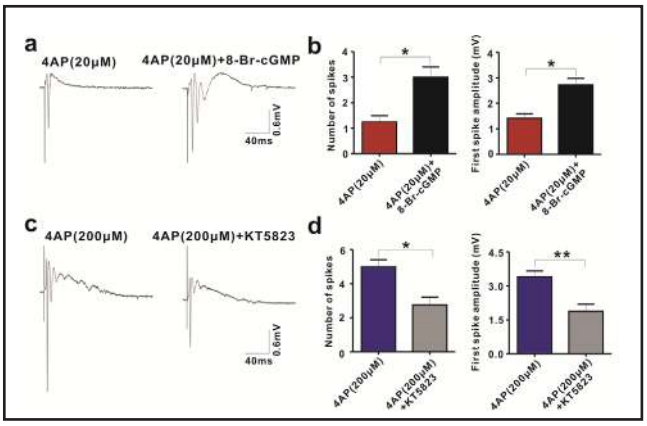

Fig. 4. Effects of cGKII activation or inhibition on stimulus-evoked population spikes in the pyramidal cell layer of CA1. Epileptiform activity was elicited by the addition of 4AP to ACSF. Population spikes in the CA1 pyramidal cell layer were observed in response to Schaffer collateral stimulation by a tungsten electrode under the following pharmacological conditions: 8-Br-cGMP (a) and KT5823 (c). (b) Effects of 8-Br-cGMP on the number of population spikes and the amplitude of the first population spike in the presence of 4AP (20 μM). (d) Effects of KT5823 on the number of population spikes and the amplitude of the first population spike in the presence of 4AP (200 μM). The significance (n = 5 slices per condition, *p<0.05, **p<0.01) was determined using Student's t-test.

cGKII was expressed primarily in postsynaptic membranes in the brain tissues of epileptic patients and rats

We subsequently performed immunofluorescence studies to detect the cellular location of cGKII in epileptic humans and rats and found that cGKII was co-expressed with the neuron-specific marker MAP2 (Figs. 1d-f) in both human and rat brain tissues, but no overlap with the astrocyte-specific marker GFAP was observed (Figs. 1g-i). These results showed that cGKII was expressed primarily in neurons but not in astrocytes, suggesting that cGKII might exert more direct effects on neurons than on astrocytes. Further immunofluorescence staining showed that cGKII was co-expressed with the postsynaptic marker PSD95 but not with the presynaptic marker vGlut1 in the hippocampus and cortex of rats (Fig. 2). Immunofluorescence staining revealed that cGKII immunoreactivity was primarily evident in postsynaptic membranes in the central nervous system.

In vivo cGKII intervention modified the severity of pilocarpine-induced seizures

The rat pilocarpine-induced seizure model was used to detect the effect of cGKII on seizure activities using various acute cGKII interventions administered via an intracerebroventricular injection of the cGKII agonist 8-Br-cGMP (500 μM), the inhibitor KT5823 (2 μM), or control solvents. First, the Racine score was recorded every 10 minutes for 60 minutes after pilocarpine injection. Repeated-measures ANOVA showed that seizure severity did not show a significant difference between the two solvent control groups at each 10-minute interval ($p = 0.822$). Compared with the two control groups, the seizures in the agonist group were more severe (**$p < 0.01$), whereas the seizures in the inhibitor group were less severe (*$p < 0.05$, Fig. 3b). A significant effect of time ($p < 0.05$) was observed, and no significant interaction between time and group was found ($p > 0.05$). Second, we found that 83.33% of the rats exhibited generalized tonic-clonic seizures (GTCSs, Racine score ≥ 4) in the two solvent control groups, whereas only 33.33% of the rats exhibited GTCSs in the inhibitor group. However, all the rats in the agonist group developed GTCSs (Fig. 3c). We subsequently measured the latency of seizure onset in the rat pilocarpine model. The results revealed that latency was notably shortened in the 8-Br-cGMP group, but no significant difference was observed between the KT5823 group and the control group (44.45 ± 1.67 min in the artificial cerebrospinal fluid (ACSF) group, 45.64 ± 2.87 min in the DMSO group, 48.55 ± 1.84 min in the KT5823 group, and 17.63 ± 1.83 min in the 8-Br-cGMP group, **$p < 0.01$, Fig. 3d). Electroencephalogram (EEG) recordings confirmed the above-mentioned results of the behavior tests (Fig. 3a). Based on the findings, we concluded that cGKII regulated pilocarpine-induced seizures: the activation of cGKII by 8-Br-cGMP increased the seizure severity and shortened the seizure latency, whereas the inhibition of cGKII by KT5823 significantly reduced the seizure severity.

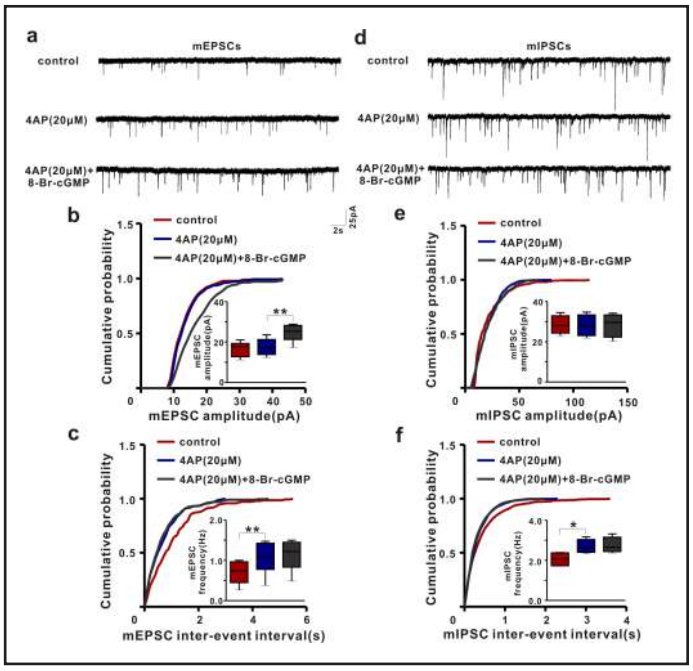

Fig. 5. 8-Br-cGMP increases the amplitude of spontaneous mEPSCs in CA1 pyramidal neurons. Sample traces of mEPSCs (a) and mIPSCs (d). Cumulative probability plots of mEPSC (b) and mIPSC (e) amplitudes. The insets display box plots of the amplitudes (mEPSCs: n = 6 cells; mIPSCs: n = 5 cells). Cumulative probability plots of mEPSC (c) and mIPSC (f) frequencies. The cumulative probabilities were measured by inter-event intervals. The insets display box plots of the actual frequencies. The significance (*p<0.05, **p<0.01) was evaluated with a KS-test (cumulative probability plots) and Student's t-test (box plots). The box plots represent the medians and inter-quartile ranges; the vertical lines represent the 10–90th percentiles.

In vitro cGKII intervention modulated 4AP-induced epileptiform discharges

4AP is one of the most popular pro-convulsant agents and exerts a significant epileptogenic effect both *in vivo* and *in vitro* [24, 26]. In addition, several studies have shown that 4AP has a significant epileptogenic effect on the hippocampal CA1 region [24, 25]. The hippocampus is closely related to epilepsy [27], and the entorhinal cortex is thought to be involved in hippocampal seizure development [28, 29]. Therefore, using 2-week-old male SD rats, we prepared hippocampal slices containing adjacent entorhinal cortex tissue and successfully induced epileptiform activity through the bath application of 4AP [22, 27]. Under our experimental conditions, we could record epileptiform discharges in the CA1 region 10 minutes after 4AP (200 μM) was applied to brain slices. 4AP (100 μM or 40 μM) could also induce epileptiform discharges, but the success rate was lower. After application of a low concentration of 4AP (20 μM), neither the extracellular field recording nor the intracellular action potential recording could detect epileptiform discharges. Because a high concentration of 4AP (200 μM) resulted in a strong pro-convulsion effect, this high concentration might mask the influence of cGKII activation on the seizure phenotype when determining whether cGKII activation has a pro-convulsion effect. Therefore, to study the effect of cGKII activation on the seizure phenotype, we applied a low concentration of 4AP (20 μM) to brain slices.

To evaluate the role of cGKII in the modulation of neural network excitability, we measured stimulus-evoked population spikes in the hippocampal CA1 region as described previously [30]. ACSF containing 4AP (20 μM or 200 μM) was superfused for 10 minutes to trigger epileptiform activity, and population spikes were then evoked. The cGKII agonist 8-Br-cGMP (500 μM) or inhibitor KT5823 (2 μM) was then superfused for 20 minutes. After the application of 4AP (20 μM), 8-Br-cGMP induced epileptiform discharges, the number of population spikes increased [1.25 ± 0.25 in the 4AP (20 μM) group, 3.00 ± 0.41 in the 4AP (20 μM) + 8-Br-cGMP group, *p < 0.05], and the amplitudes of the first population spikes increased [1.42 ± 0.17 in the 4AP (20 μM) group, 2.73 ± 0.25 in the 4AP (20 μM) + 8-Br-cGMP group, *p < 0.05, Figs. 4a, b]. In contrast, epileptiform activity was successfully triggered after 4AP (200 μM) was added to the bath solution, and KT5823 suppressed 4AP-induced epileptiform discharges (*p < 0.05, **p < 0.01, Figs. 4c, d).

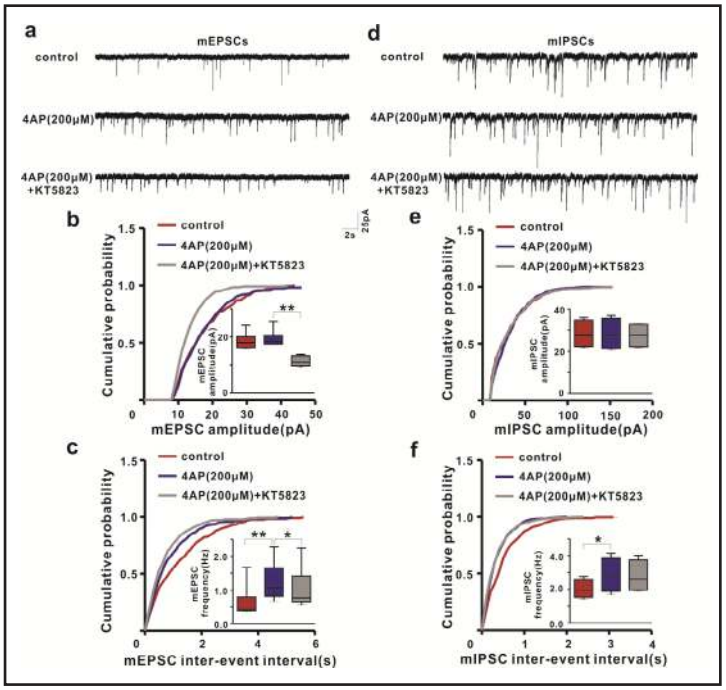

Fig. 6. KT5823 reduces the amplitude and frequency of spontaneous mEPSCs in CA1 pyramidal neurons. Sample traces of mEPSCs (a) and mIPSCs (d). Hippocampal slices were sequentially perfused with the solutions in the absence (control) and presence of 4AP (200 μM) and 4AP (200 μM) + KT5823. Cumulative probability plots of mEPSC (b) and mIPSC (e) amplitudes. The insets display box plots of the amplitudes (mEPSCs: n = 6 cells; mIPSCs: n = 5 cells). Cumulative probability plots of mEPSC (c) and mIPSC (f) frequencies. The cumulative probabilities were measured by the inter-event intervals. The insets display box plots of the actual frequencies. The significance (*p<0.05, **p<0.01) was evaluated with a KS-test (cumulative probability plots) and Student's t-test (box plots). The box plots represent the medians and inter-quartile ranges, and the vertical lines represent the 10–90th percentiles.

Using whole-cell current-patch clamp recordings, we further explored whether cGKII could change neuronal excitability at the cellular level. Under stimulation with the epileptogenic factor 4AP (20 μM), the activation of cGKII by 8-Br-cGMP (500 μM) triggered paroxysmal depolarization shifts (PDSs) in pyramidal neurons in the hippocampal CA1 region. PDSs are typical of epileptiform activity, which is displayed primarily as a burst of high-frequency action potential (at least four action potentials occur in a PDS) [31]. To verify that these epileptiform discharges were truly caused by 8-Br-cGMP, we washed the brain slices with ACSF containing 4AP (20 μM) at the end of the experiment and found that the epileptiform discharges nearly disappeared (Fig. 3e). Due to the hyperexcitability of neurons under stimulation with epileptogenic agents, the burst frequency of action potentials, the frequency of PDSs, and the burst frequency of action potentials in PDSs could be measured to assess seizure severity [31]. Therefore, we calculated the following three parameters: the mean firing frequency [0.67 ± 0.14 Hz in the 4AP (20 μM) group, 1.27 ± 0.18 Hz in the 4AP (20 μM) + 8-Br-cGMP group, and 0.78 ± 0.09 Hz in the washout group, **p < 0.01, Fig. 3f], the mean frequency of PDSs [no PDSs in the 4AP (20 μM) group, 0.09 ± 0.02 Hz in the 4AP (20 μM) + 8-Br-cGMP group, and 0.02 ± 0.01 Hz in the washout group, **p < 0.01, Fig. 3g], and the average action potential in the PDSs [6.85 ± 1.05 Hz in the 4AP (20 μM) + 8-Br-cGMP group, 5.01 ± 0.31 Hz in the washout group, *p < 0.05, Fig. 3h]. After perfusion of the brain slices with a high concentration of 4AP (200 μM), more than 70% of the hippocampal CA1 neurons successfully induced epileptiform discharges. We also found that KT5823 significantly suppressed epileptiform activity under epileptogenic stimulation with 4AP (200 μM, Fig. 3i). KT5823 reduced the mean firing frequency (1.26 ± 0.14 Hz) compared with that in the control epileptic group (2.99 ± 0.32 Hz, **p < 0.01, Fig. 3j), and washing the slices with ACSF containing 4AP (200 μM) restored the mean firing frequency was restored (2.34 ± 0.30 Hz, *p < 0.05, Fig. 3j). KT5823 could also reduce the mean frequency of PDSs [0.22 ± 0.04 Hz in the 4AP (200 μM) group, 0.03 ± 0.005 Hz in the 4AP (200 μM) + KT5823 group, and 0.14 ± 0.01 Hz in the washout group, **p < 0.01, Fig. 3k] and the average action potential in PDSs [7.84 ± 0.69 Hz in the 4AP (200 μM) group, 4.57 ± 0.16 Hz in the 4AP (200 μM) + KT5823

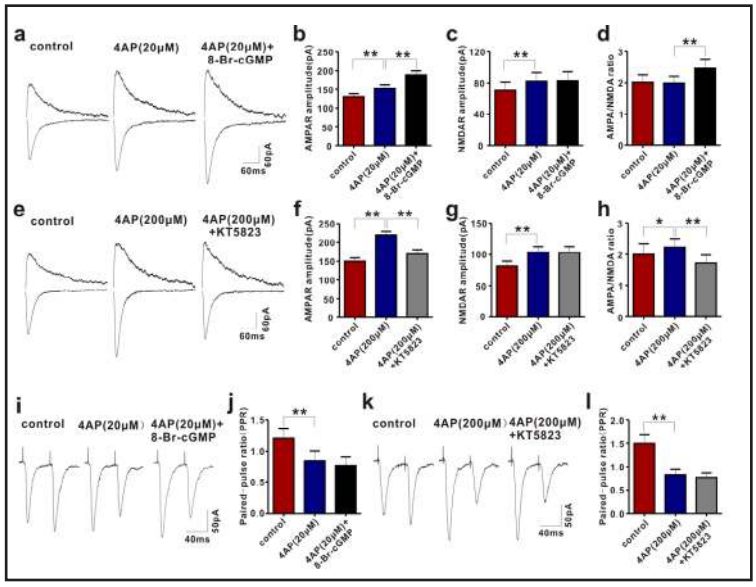

Fig. 7. 8-Br-cGMP and KT5823 treatment impairs AMPA receptor-mediated synaptic responses in hippocampal CA1 pyramidal neurons. Sample traces of AMPA and NMDA receptor-mediated synaptic responses (a and e). Pooled data showing the AMPAR-mediated synaptic responses (b and f), NMDAR-mediated synaptic responses (c and g), and AMPA/NMDA ratio (d and h) (n = 6 cells). Representative traces of evEPSCs in response to paired-pulse stimulation at an inter-pulse interval of 50 ms (i and k). (j) The histogram shows the mean PPR before and after the application of 4AP (20 μM) or 8-Br-cGMP (n = 5 cells). (l) The histogram shows the mean PPR before and after the application of 4AP (200 μM) or KT5823 (n = 5 cells). The significance (*p<0.05, **p<0.01) was determined using Student's t-test.

group, and 6.67 ± 0.88 Hz in the washout group, *p < 0.05, **p < 0.01, Fig. 3l]. These results suggested that cGKII activation could induce the seizure phenotype in the presence of a subthreshold dose of 4AP and that cGKII inhibition suppressed epileptiform activity when a high concentration of 4AP successfully triggered epileptiform activity. These findings were consistent in the extracellular and intracellular recordings.

cGKII intervention altered excitatory synaptic transmission but did not affect inhibitory synaptic transmission

To explore the underlying mechanism through which cGKII affected 4AP-induced epileptiform activity, whole-cell voltage-patch clamp recordings were performed to detect whether cGKII intervention could change the miniature excitatory postsynaptic currents (mEPSCs) and the miniature inhibitory postsynaptic currents (mIPSCs) in hippocampal CA1 pyramidal neurons. The perfusion of brain slices with 4AP (20 or 200 μM) significantly increased the frequencies of both mEPSCs and mIPSCs, but the amplitudes of mEPSCs and mIPSCs were not significantly affected (*p < 0.05, **p < 0.01, Fig. 5 and Fig. 6). Under stimulation with 4AP (20 μM), bath application of 8-Br-cGMP significantly increased the amplitude of mEPSCs [17.49 ± 1.71 pA in the 4AP (20 μM) group, 24.56 ± 1.76 pA in the 4AP (20 μM) + 8-Br-cGMP group, **p < 0.01, Fig. 5b] but did not significantly affect the frequency of mEPSCs (p > 0.05, Fig. 5c). 8-Br-cGMP had no effect on neither the amplitude nor the frequency of mIPSCs (p > 0.05, Figs. 5e and f). In contrast, after application of 4AP (200 μM), KT5823 significantly reduced both the amplitude and the frequency of mEPSCs [amplitude: 19.24 ± 1.27 pA in the 4AP (200 μM) group, 11.30 ± 0.77 pA in the 4AP (200 μM) + KT5823 group; frequency: 1.23 ± 0.24 Hz in the 4AP (200 μM) group, 1.02 ± 0.26 Hz in the 4AP (200 μM) + KT5823 group; *p < 0.05, **p < 0.01, Figs. 6a-c]. However, this treatment did not significantly affect the amplitude or the frequency of mIPSCs (p > 0.05, Figs. 6d-f). These results suggested that the activation or inhibition of cGKII under stimulation with an epileptogenic factor significantly affected excitatory synaptic transmission in hippocampal CA1 pyramidal neurons but did not affect inhibitory synaptic transmission.

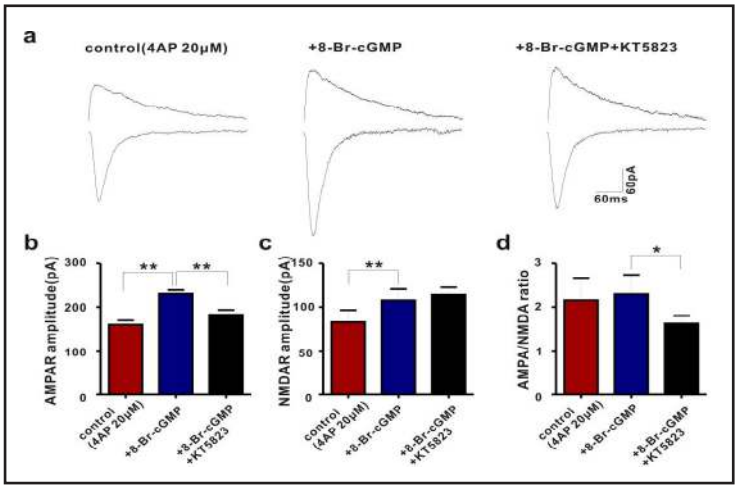

Fig. 8. KT5823 treatment reduces the effect of 8-Br-cGMP. Sample traces of AMPA and NMDA receptor-mediated synaptic responses in the control condition (4AP 20 μM), in the presence of 8-Br-cGMP, and in the presence of 8-Br-cGMP + KT5823 (a). Pooled data demonstrating the AMPAR-mediated synaptic responses (b), NMDAR-mediated synaptic responses (c), and the AMPA/NMDA ratio (d) (n = 5 cells). The significance (*p<0.05, **p<0.01) was determined using Student's t-test.

cGKII affected AMPAR-mediated excitatory synaptic transmission through a postsynaptic mechanism

To understand the mechanism through which cGKII affects excitatory synaptic transmission, we first referred to previously described experimental methods [32] and measured the glutamatergic synaptic strength by examining the AMPA/NMDA ratio. The exposure of brain slices to a low concentration of 4AP (20 μM) could increase AMPAR- and NMDAR-mediated EPSC amplitudes (**p < 0.01), but the AMPA/NMDA ratio did not change significantly (p > 0.05, Figs. 7a-d). The bath application of 8-Br-cGMP increased the AMPA/NMDA ratio [1.99 ± 0.21 in the 4AP (20 μM) group, 2.47 ± 0.29 in the 4AP (20 μM) + 8-Br-cGMP group, **p < 0.01, Fig. 7d], which was prompted by a significant increase in the amplitude of AMPAR-mediated evoked excitatory postsynaptic currents (evEPSCs) [153.10 ± 9.55 in the 4AP (20 μM) group, 189.29 ± 10.60 in the 4AP (20 μM) + 8-Br-cGMP group, **p < 0.01, Fig. 7b]. The amplitude of NMDAR-mediated evEPSCs did not change significantly [82.23 ± 11.48 in the 4AP (20 μM) group, 82.86 ± 11.89 in the 4AP (20 μM) + 8-Br-cGMP group, Fig. 7c]. The application of a high concentration of 4AP (200 μM) to the brain slices increased the AMPA/NMDA ratio (*p < 0.05, Fig. 7h), and this effect might have been obtained because the high concentration of 4AP enhanced the amplitude of the AMPAR-mediated current to a higher level compared with that of the NMDAR-mediated current. Based on the high concentration of 4AP, we applied KT5823 and found that the AMPA/NMDA ratio was reduced [2.22 ± 0.28 in the 4AP (200 μM) group, 1.73 ± 0.25 in the 4AP (200 μM) + KT5823 group, **p < 0.01, Fig. 7h], resulting in a reduction in the amplitude of AMPAR-mediated evEPSCs [219.87 ± 9.15 in the 4AP (200 μM) group, 169.51 ± 10.92 in the 4AP (200 μM) + KT5823 group, **p < 0.01, Fig. 7f] with no significant change in the amplitude of NMDAR-mediated evEPSCs [103.66 ± 8.94 in the 4AP (200 μM) group, 103.50 ± 9.12 in the 4AP (200 μM) + KT5823 group, Fig. 7g)]. The data showed that 8-Br-cGMP induced an increase in AMPAR-mediated evEPSCs, and this effect was then partially blocked by the addition of KT5823 (Fig. 8). These results suggested that a low concentration of 4AP enhanced the glutamatergic synaptic strength and that the activation of cGKII further enhanced the glutamatergic synaptic strength by increasing AMPAR-mediated evEPSCs. In addition, KT5823 could partially prevent the effect of 8-Br-cGMP. In contrast, a high concentration of 4AP significantly enhanced the glutamatergic synaptic strength. The inhibition of cGKII significantly reduced AMPAR-mediated evEPSCs, thereby weakening the strength of excitatory synapses.

To further explore whether the alteration in the AMPA/NMDA ratio due to cGKII was caused by the release of presynaptic excitatory neurotransmitters, we determined the paired-pulse EPSC ratio (PPR) according to previously described methods [33]. A significant decrease in the PPR was observed after 4AP application (20 or 200 μM) compared with that in the control group (**p < 0.01, Figs. 7i-l), indicating that 4AP increased the presynaptic

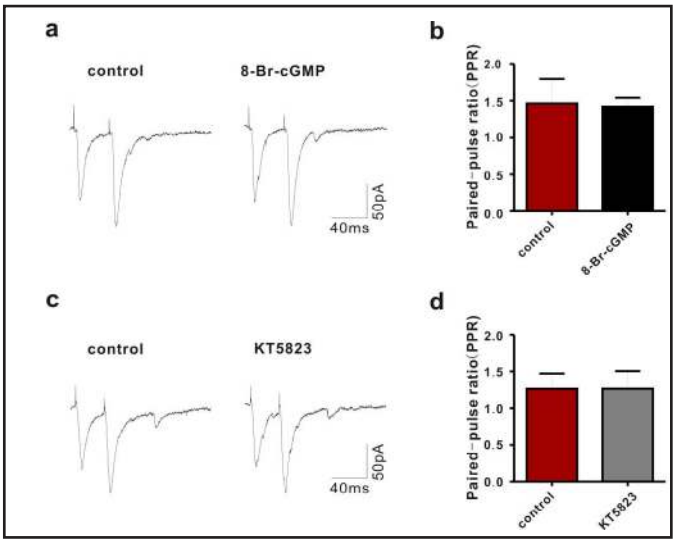

Fig. 9. Effects of 8-Br-cGMP and KT5823 on the PPR. Representative traces of evEPSCs in response to paired-pulse stimulation at an inter-pulse interval of 50 ms (a and c). (b) The histogram shows the mean PPRs before and after the application of 8-Br-cGMP (n = 5 cells). (d) The histogram shows the mean PPRs before and after the application of KT5823 (n = 5 cells). The significance was determined using Student's t-test.

release probability. However, neither the activation nor the inhibition of cGKII significantly changed the PPR compared with the epileptic condition ($p > 0.05$, Figs. 7i-l). Similarly, we applied 8-Br-cGMP and KT5823 directly to brain slices and observed no significant changes in the PPRs, regardless of the agonism or inhibition of cGKII ($p > 0.05$, Fig. 9), indicating that the cGKII-mediated alteration of the AMPA/NMDA ratio was not due to changes in the presynaptic release probability. Therefore, we hypothesized that this change might be a consequence of changes in postsynaptic AMPAR function.

cGKII modulated AMPAR-mediated excitatory synaptic transmission by regulating the composition of calcium-permeable AMPARs

To investigate the possible processes involved in the change in AMPAR function, we measured the current-voltage (I-V) relationships in AMPAR-mediated currents in the hippocampal CA1 area. We recorded AMPAR-mediated evEPSCs at different holding potentials (-60 mV, -40 mV, -20 mV, 0 mV, +20 mV, and +40 mV) using a pipette solution containing spermine (100 μM) as described previously [34]. The rectification index (RI) was calculated by dividing the average amplitude of the evEPSCs measured at a holding potential of -60 mV by that measured at +40 mV. We found that the AMPAR-mediated I-V curve was relatively linear when a low concentration of 4AP (20 μM) was applied to brain slices. Subsequent application of 8-Br-cGMP caused the IV curve to exhibit rectifying properties and significantly heightened the AMPA RI [1.91 ± 0.13 in the 4AP (20 μM) group, 3.31 ± 0.14 in the 4AP (20 μM) + 8-Br-cGMP group, $^{**}p < 0.01$, Figs. 10a-c]. In contrast, the AMPA RI was significantly decreased after KT5823 treatment compared with that in the 4AP (200 μM) control group [1.96 ± 0.13 in the 4AP (200 μM) group, 1.48 ± 0.09 in the 4AP (200 μM) + KT5823 group, $^{**}p < 0.01$, Figs. 10d-f]. The RI reflects an alteration in the number of GluA2-lacking calcium-permeable AMPARs on the membrane. Taken together, these findings suggested that the alteration of AMPAR-mediated excitatory synaptic transmission by cGKII intervention might be caused by changes in the synaptic delivery of GluA2-lacking calcium-permeable AMPARs.

To verify the above conclusion, we applied IEM1460 (50 μM), a specific inhibitor of calcium-permeable AMPARs, to investigate whether cGKII activation could still increase the AMPA/NMDA ratio. The results revealed that IEM1460 significantly decreased the AMPA/NMDA ratio compared with that in the 4AP (20 μM) control group ($^{**}p < 0.01$, Fig. 10h). The addition of 8-Br-cGMP to the perfusion solution to activate cGKII did not significantly change the AMPA/NMDA ratio [2.15 ± 0.18 in the 4AP (20 μM) group, 1.65 ± 0.16 in the IEM1460 group, and 1.64 ± 0.18 in the IEM1460 + 8-Br-cGMP group, $p > 0.05$, Figs. 10g, h]. These results further demonstrated that cGKII activation increased the synaptic delivery of GluA2-lacking calcium-permeable AMPARs.

cGKII regulated the synaptic delivery of GluA1 by phosphorylating GluA1 at Ser845 and was unaffected by the PKA (cAMP-dependent protein kinase) pathway

Previous studies have shown that approximately 80% of AMPARs in the hippocampus are GluA1/GluA2 heteromers [35] and that the delivery of GluA1 to the membrane is regulated primarily by GluA1 phosphorylation at Ser845 [36]. Our study showed that cGKII regulated the composition of GluA2-lacking calcium-permeable AMPARs at the postsynaptic membrane. Therefore, we hypothesized that cGKII activation might strengthen the synaptic delivery of GluA1 by phosphorylating GluA1 at Ser845 to promote seizures. To verify this hypothesis, we added the GluA1 inhibitory peptide TLPRNSGAG (-SGAG, 200 μM), which inhibits GluA1 at Ser845, and a control peptide NRPGGTLSA (-TLSA, 200 μM) to the pipette solution and then investigated whether the activation of cGKII could increase the AMPA/NMDA ratio. The results showed that 8-Br-cGMP could increase the AMPA/NMDA ratio in the control peptide group compared with that in the 4AP (20 μM) control group (1.74 ± 0.25 in the control group, 2.27 ± 0.22 in the 8-Br-cGMP group, **p < 0.01, Figs. 10i, l). However, no significant change in the AMPA/NMDA ratio was observed in the inhibitory peptide group after 8-Br-cGMP treatment (2.20 ± 0.17 in the control group, 2.19 ± 0.18 in the 8-Br-cGMP group, Figs. 10j and l). These results indicated that cGKII strengthened excitatory synaptic transmission primarily by phosphorylating GluA1 at Ser845 to increase calcium-permeable AMPARs in postsynaptic

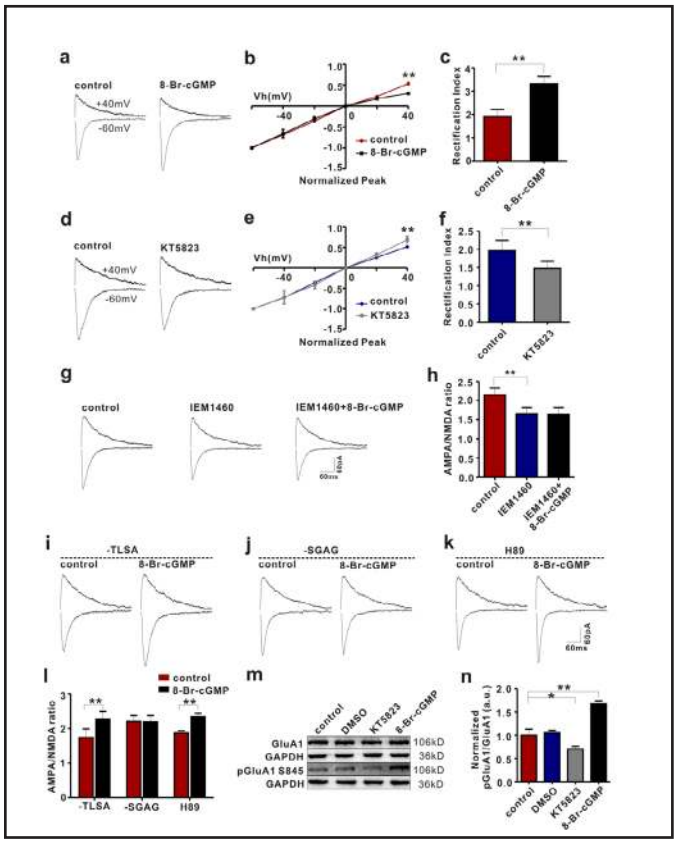

Fig. 10. cGKII intervention impairs calcium-permeable AMPARs, and this effect is mediated by the phosphorylation of GluA1 at S845 and is not affected by PKA. (a and d) Representative AMPAR-mediated synaptic responses (AMPA EPSCs) recorded at -60 mV and +40 mV (Vh) in rat slices. (b) The current-voltage plot (I/V curve) of the control group exhibited a linear I-V relationship, but the 8-Br-cGMP group exhibited an inwardly rectifying I-V relationship. (c) Pooled data showing that the AMPA receptor RI in the 8-Br-cGMP group was significantly increased compared with that in the control group (n = 6 cells). (e) I/V curves obtained from the control and KT5823 groups. (f) Pooled data showing the decrease in the RI following KT5823 treatment (n = 6 cells). (g and h) Effects of IEM1460 and 8-Br-cGMP on the AMPA/NMDA ratio (n = 6 cells). Hippocampal slices were sequentially perfused with the following external solutions: 4AP (20 μM) and 4AP (20 μM) + 8-Br-cGMP. Additionally, the pipette solution contained the GluA1-Ser845 scrambled peptide TLSA (i), the inhibitory peptide SGAG (j), or the PKA inhibitor H89 (k). (l) Pooled data showing that 8-Br-cGMP could not increase the AMPA/NMDA ratio in the presence of the inhibitory peptide, but after inhibition of the PKA pathway with H89, 8-Br-cGMP could increase the AMPA/NMDA ratio (n = 6 cells). (m and n) The levels of total GluA1 and phosphorylated GluA1 at S845 (pGluA1) were assayed by western blot (n = 6). The significance (*p<0.05, **p<0.01) was evaluated by Student's t-test or one-way ANOVA.

membranes. Similarly, *in vivo*, rats were subjected to acute activation or inhibition of cGKII via the intracerebroventricular injection of 8-Br-cGMP or KT5823, respectively, and were then administered an intraperitoneal pilocarpine injection to induce seizures. One hour after seizure onset, the rats' brains were removed, and western blots were performed to detect the levels of total GluA1 and pGluA1-Ser845. Compared with the two control groups, the expression of total GluA1 in the KT5823 group and the 8-Br-cGMP group was not significantly changed ($p > 0.05$). However, the expression of pGluA1-Ser845 was significantly upregulated in the 8-Br-cGMP group ($^{**}p < 0.01$) and decreased in the KT5823 group ($^{*}p < 0.05$, Figs. 10m, n). These results suggested that cGKII could regulate the phosphorylation of GluA1 at Ser845 both *in vivo* and *in vitro* under stimulation with epileptogenic agents.

Because the PKA pathway might also regulate the transportation of GluA1 to the membrane by phosphorylating GluA1 at Ser845 [37], whole-cell patch-clamp recordings were performed to determine whether the cGKII-induced modulation of seizures by the phosphorylation of GluA1 at Ser845 was affected by the PKA pathway. The PKA pathway inhibitor H89 (10 μM) was added to the pipette solution to determine whether cGKII activation could still increase the AMPA/NMDA ratio, and we found that 8-Br-cGMP increased the AMPA/NMDA ratio after inhibition of the PKA pathway by H89 (1.87 ± 0.06 in the control group, 2.34 ± 0.11 in the 8-Br-cGMP group, $^{**}p < 0.01$, Figs. 10k, l). These results suggested that the cGKII-regulated postsynaptic membrane delivery of GluA1 by Ser845 phosphorylation is involved in seizures and is not affected by the PKA pathway.

Discussion

TLE is the most common and most devastating form of intractable epilepsy. At present, there is no effective drug for controlling TLE; therefore, the identification of a therapeutic target has become a focus of epilepsy research. Emerging evidence suggests that multiple mechanisms are involved in the development of epilepsy; however, these mechanisms eventually lead to a common pathophysiological change, namely, an imbalance between excitation and inhibition in the central nervous system [5]. AMPARs, which mediate the majority of fast excitatory synaptic transmissions, are highly dynamic, and alterations in their number, subunit composition, and phosphorylation state can regulate synaptic strength [38]. GluA1 is an important subunit of AMPARs, and its increased expression at the postsynaptic membrane can strengthen synaptic transmission and function in seizures [12, 39]. The phosphorylation of GluA1 might facilitate its transfer to the postsynaptic membrane [40]. PKA can promote the anchoring of GluA1 to the cell membrane through the phosphorylation of GluA1 at Ser845. Recent studies have shown that cGKII can produce a similar effect through the phosphorylation of GluA1 at Ser845 [17, 18]. These findings led us to hypothesize that cGKII dysfunction is involved in epilepsy. We used pilocarpine and 4AP to construct seizure models and performed molecular biology assays, behavioral tests, and electrophysiology assays to validate this hypothesis and to further explore the potential associated mechanisms.

This study provides the first demonstration that cGKII plays a critical role in epileptic seizures. In particular, we found that cGKII expression was upregulated in the brain tissues of patients with drug-resistant epilepsy compared with that in the brain tissues of control patients, whereas the expression of cGKI, a cGK isoform, in epileptic patients was not significantly different. Moreover, in a rat pilocarpine-induced epilepsy model, we also found that the expression of cGKII, but not cGKI, was significantly increased in the temporal cortex and hippocampus. Double immunofluorescence staining of epileptic brain tissues revealed that cGKII was expressed primarily in neurons and not in astrocytes, which suggests that it exerts a more direct effect on neurons compared with astrocytes. Further immunofluorescence staining indicated that cGKII was primarily present at the postsynaptic membrane, suggesting that cGKII might be involved in the modulation of synaptic strength. Taken together, these results show that cGKII might be involved in epileptic seizures.

To verify whether cGKII is involved in the regulation of epileptic seizures, we injected the cGKII agonist 8-Br-cGMP or its inhibitor KT5823 intracerebroventricularly and then used pilocarpine to construct an acute seizure model. Our results showed that the activation of cGKII aggravated the severity of seizures, shortened the latency to first-seizure onset, and increased the incidence of GTCSs. In contrast, cGKII inhibition attenuated seizure severity, but no significant difference in onset latency was observed compared with the control group. These results support our hypothesis that cGKII dysfunction is involved in epilepsy. To further validate this conclusion, we applied 4AP to induce epileptiform activity *in vitro* and found that a low concentration of 4AP could not trigger epileptiform activity but could induce an increase in excitability. However, the activation of cGKII resulted in the appearance of obvious epileptiform discharges, indicating that cGKII activation could decrease the threshold of 4AP-induced epileptiform activity. In contrast, a high concentration of 4AP successfully triggered epileptiform activity. The suppression of cGKII by KT5823 decreased the severity of epileptiform activity in both extracellular and intracellular recordings. These results further confirmed that cGKII dysfunction is involved in epileptic seizures.

To investigate the mechanism underlying this effect, whole-cell patch-clamp recordings were performed to study the effect of cGKII on the excitability of hippocampal CA1 pyramidal neurons. First, we found that the effect of cGKII on epileptiform discharges was due to damage to glutamatergic synaptic transmission. Both excitatory synaptic transmission and inhibitory synaptic transmission in hippocampal CA1 pyramidal neurons were enhanced after treatment with a low concentration of 4AP. The activation of cGKII enhanced excitatory synaptic transmission, but not inhibitory synaptic transmission, leading to a further increase in neuronal excitability that could lead to seizures. We subsequently found that cGKII activation had no significant influence on the excitatory synaptic PPR, increased the AMPA/NMDA ratio and AMPAR-mediated currents, and did not change the NMDAR-mediated currents, suggesting that cGKII activation could strengthen excitatory synaptic transmission most likely by enhancing the expression and function of postsynaptic AMPARs. In contrast, cGKII inhibition significantly reduced AMPAR-mediated excitatory synaptic transmission, reducing the excitotoxicity of a high concentration of 4AP through postsynaptic mechanisms.

We further performed electrophysiological studies on hippocampal CA1 pyramidal neurons and found that cGKII activation enhanced the RI of AMPARs, whereas the inwardly rectifying property of AMPARs was mediated by calcium permeability [41]. The blockage of calcium-permeable AMPARs by IEM1460 revealed that cGKII activation could no longer increase the AMPA/NMDA ratio, which further verified that cGKII played a critical role in regulating calcium-permeable AMPARs. Previous studies revealed that AMPARs in the hippocampus are primarily composed of GluA1 and GluA2, that calcium-permeable AMPARs are GluA2-lacking AMPARs, and that GluA1 delivery to the membrane is regulated primarily by the phosphorylation of GluA1 at Ser845. Our results revealed that cGKII was expressed primarily in the postsynaptic membrane. Therefore, we speculated that cGKII regulated GluA1 expression on the postsynaptic membrane primarily by phosphorylating GluA1 at Ser845 to modulate calcium-permeable AMPARs. We applied inhibitory and control peptides of GluA1 phosphorylation at Ser845 to the pipette solution and found that cGKII activation could still increase the AMPA/NMDA ratio in the control peptide group, but this effect was not observed in the inhibitory peptide group. Because the PKA pathway also affected the phosphorylation of GluA1 at Ser845, we applied H89 to block the PKA pathway and found that cGKII activation could still increase the AMPA/NMDA ratio. We concluded that the effect of cGKII on GluA1 was not affected by the PKA pathway.

In summary, our results confirm the hypothesis that cGKII is involved in the regulation of seizures and further demonstrate that the underlying mechanism through which cGKII regulates AMPAR-mediated synaptic transmission involves the phosphorylation of GluA1 at Ser845, which modulates the expression and function of GluA1 in the postsynaptic membrane. Therefore, cGKII is involved in the regulation of seizures, which suggests that cGKII might be a new potential therapeutic target for epilepsy.

Acknowledgements

This work was supported by the National Natural Science Foundation of China (grant numbers 81471319, 81301110, 81671301, and 81701280). We sincerely appreciate Beijing Tiantan Hospital and Xuanwu Hospital of the Capital University of Medical Sciences for supplying the surgical brain samples. In addition, we thank the patients and their families for their voluntary participation in this study.

Disclosure Statement

The authors declare no competing financial interests.

References

1 Ngugi AK, Bottomley C, Kleinschmidt I, Sander JW, Newton CR: Estimation of the burden of active and life-time epilepsy: a meta-analytic approach. Epilepsia 2010;51:883-890.
2 Kwan P, Arzimanoglou A, Berg AT, Brodie MJ, Allen Hauser W, Mathern G, Moshe SL, Perucca E, Wiebe S, French J: Definition of drug resistant epilepsy: consensus proposal by the ad hoc Task Force of the ILAE Commission on Therapeutic Strategies. Epilepsia 2010;51:1069-1077.
3 Cascino GD: Temporal lobe epilepsy is a progressive neurologic disorder: Time means neurons! Neurology 2009;72:1718-1719.
4 Nevalainen O, Ansakorpi H, Simola M, Raitanen J, Isojarvi J, Artama M, Auvinen A: Epilepsy-related clinical characteristics and mortality: a systematic review and meta-analysis. Neurology 2014;83:1968-1977.
5 Scharfman HE: The neurobiology of epilepsy. Curr Neurol Neurosci Rep 2007;7:348-354.
6 Rogawski MA: AMPA receptors as a molecular target in epilepsy therapy. Acta Neurol Scand Suppl 2013;197:S9-18.
7 Zaccara G, Giovannelli F, Cincotta M, Iudice A: AMPA receptor inhibitors for the treatment of epilepsy: the role of perampanel. Expert Rev Neurother 2013;13:647-655.
8 Zhang J, Abdullah JM: The role of GluA1 in central nervous system disorders. Rev Neurosci 2013;24:499-505.
9 Rakhade SN, Zhou C, Aujla PK, Fishman R, Sucher NJ, Jensen FE: Early alterations of AMPA receptors mediate synaptic potentiation induced by neonatal seizures. J Neurosci 2008;28:7979-7990.
10 Plant K, Pelkey KA, Bortolotto ZA, Morita D, Terashima A, McBain CJ, Collingridge GL, Isaac JTR: Transient incorporation of native GluR2-lacking AMPA receptors during hippocampal long-term potentiation. Nature Neuroscience 2006;9:602-604.
11 Lopes MW, Soares FM, de Mello N, Nunes JC, Cajado AG, de Brito D, de Cordova FM, da Cunha RM, Walz R, Leal RB: Time-dependent modulation of AMPA receptor phosphorylation and mRNA expression of NMDA receptors and glial glutamate transporters in the rat hippocampus and cerebral cortex in a pilocarpine model of epilepsy. Exp Brain Res 2013;226:153-163.
12 Rajasekaran K, Todorovic M, Kapur J: Calcium-permeable AMPA receptors are expressed in a rodent model of status epilepticus. Ann Neurol 2012;72:91-102.
13 Hofmann F, Wegener JW: cGMP-dependent protein kinases (cGK). Methods Mol Biol 2013;1020:17-50.
14 el-Husseini AE, Bladen C, Vincent SR: Molecular characterization of a type II cyclic GMP-dependent protein kinase expressed in the rat brain. J Neurochem 1995;64:2814-2817.
15 Wincott CM, Kim S, Titcombe RF, Tukey DS, Girma HK, Pick JE, Devito LM, Hofmann F, Hoeffer C, Ziff EB: Spatial memory deficits and motor coordination facilitation in cGMP-dependent protein kinase type II-deficient mice. Neurobiol Learn Mem 2013;99:32-37.
16 Wincott CM, Abera S, Vunck SA, Tirko N, Choi Y, Titcombe RF, Antoine SO, Tukey DS, DeVito LM, Hofmann F, Hoeffer CA, Ziff EB: cGMP-dependent protein kinase type II knockout mice exhibit working memory impairments, decreased repetitive behavior, and increased anxiety-like traits. Neurobiol Learn Mem 2014;114:32-39.

17 Serulle Y, Zhang S, Ninan I, Puzzo D, McCarthy M, Khatri L, Arancio O, Ziff EB: A glur1-cgkii interaction regulates ampa receptor trafficking. Neuron 2007;56:670-688.
18 Incontro S, Ciruela F, Ziff E, Hofmann F, Sanchez-Prieto J, Torres M: The type II cGMP dependent protein kinase regulates GluA1 levels at the plasma membrane of developing cerebellar granule cells. Biochim Biophys Acta 2013;1833:1820-1831.
19 Zhang X, Chen G, Lu Y, Liu J, Fang M, Luo J, Cao Q, Wang X: Association of mitochondrial letm1 with epileptic seizures. Cereb Cortex 2014;24:2533-2540.
20 Cao Q, Wang W, Gu J, Jiang G, Wang K, Xu Z, Li J, Chen G, Wang X: Elevated expression of acid-sensing ion channel 3 inhibits epilepsy via activation of interneurons. Mol Neurobiol 2016;53:485-498.
21 Fang M, Wei JL, Tang B, Liu J, Chen L, Tang ZH, Luo J, Chen GJ, Wang XF: Neuroligin-1 Knockdown Suppresses Seizure Activity by Regulating Neuronal Hyperexcitability. Mol Neurobiol 2016;53:270-284.
22 Racine RJ: Modification of seizure activity by electrical stimulation. II. Motor seizure. Electroencephalogr Clin Neurophysiol 1972;32:281-294.
23 Paxinos G, Watson C: The rat brain in stereotaxic coordinates, 5th ed, San Diego, Elsevier, 2005.
24 Jung S, Yang H, Kim BS, Chu K, Lee SK, Jeon D: The immunosuppressant cyclosporin A inhibits recurrent seizures in an experimental model of temporal lobe epilepsy. Neurosci Lett 2012;529:133-138.
25 Toprani S, Durand DM: Fiber tract stimulation can reduce epileptiform activity in an in-vitro bilateral hippocampal slice preparation. Exp Neurol 2013;240:28-43.
26 Xu L, Rensing N, Yang XF, Zhang HX, Thio LL, Rothman SM, Weisenfeld AE, Wong M, Yamada KA: Leptin inhibits 4-aminopyridine- and pentylenetetrazole-induced seizures and AMPAR-mediated synaptic transmission in rodents. J Clin Invest 2008;118:272-280.
27 Chatzikonstantinou A: Epilepsy and the hippocampus. Front Neurol Neurosci 2014;34:121-142.
28 Gloveli T, Schmitz D, Heinemann U: Interaction between superficial layers of the entorhinal cortex and the hippocampus in normal and epileptic temporal lobe. Epilepsy Res 1998;32:183-193.
29 Scharfman HE: Epileptogenesis in the parahippocampal region. Parallels with the dentate gyrus. Ann N Y Acad Sci 2000;911:305-327.
30 Nakajima K, Yin X, Takei Y, Seog DH, Homma N, Hirokawa N: Molecular motor KIF5A is essential for GABA(A) receptor transport, and KIF5A deletion causes epilepsy. Neuron 2012;76:945-961.
31 Sah N, Rajput SK, Singh JN, Meena CL, Jain R, Sikdar SK, Sharma SS: L-pGlu-(2-propyl)-L-His-L-ProNH(2) attenuates 4-aminopyridine-induced epileptiform activity and sodium current: a possible action of new thyrotropin-releasing hormone analog for its anticonvulsant potential. Neuroscience 2011;199:74-85.
32 Etherton MR, Tabuchi K, Sharma M, Ko J, Sudhof TC: An autism-associated point mutation in the neuroligin cytoplasmic tail selectively impairs AMPA receptor-mediated synaptic transmission in hippocampus. Embo j 2011;30:2908-2919.
33 Hunt RF, Dinday MT, Hindle-Katel W, Baraban SC: LIS1 deficiency promotes dysfunctional synaptic integration of granule cells generated in the developing and adult dentate gyrus. J Neurosci 2012;32:12862-12875.
34 Gerace E, Masi A, Resta F, Felici R, Landucci E, Mello T, Pellegrini-Giampietro DE, Mannaioni G, Moroni F: PARP-1 activation causes neuronal death in the hippocampal CA1 region by increasing the expression of Ca(2+)-permeable AMPA receptors. Neurobiol Dis 2014;70:43-52.
35 Lu W, Shi Y, Jackson AC, Bjorgan K, During MJ, Sprengel R, Seeburg PH, Nicoll RA: Subunit composition of synaptic AMPA receptors revealed by a single-cell genetic approach. Neuron 2009;62:254-268.
36 Bassani S, Folci A, Zapata J, Passafaro M: AMPAR trafficking in synapse maturation and plasticity. Cell Mol Life Sci 2013;70:4411-4430.
37 Lee HK: Ca-permeable AMPA receptors in homeostatic synaptic plasticity. Front Mol Neurosci 2012;5:17.
38 Chater TE, Goda Y: The role of AMPA receptors in postsynaptic mechanisms of synaptic plasticity. Front Cell Neurosci 2014;8:401.
39 Rajasekaran K, Joshi S, Kozhemyakin M, Todorovic MS, Kowalski S, Balint C, Kapur J: Receptor trafficking hypothesis revisited: plasticity of AMPA receptors during established status epilepticus. Epilepsia 2013;54:S14-16.
40 Wang G, Gilbert J, Man HY: AMPA receptor trafficking in homeostatic synaptic plasticity: functional molecules and signaling cascades. Neural Plast 2012;2012:825364.
41 Zonouzi M, Renzi M, Farrant M, Cull-Candy SG: Bidirectional plasticity of calcium-permeable AMPA receptors in oligodendrocyte lineage cells. Nat Neurosci 2011;14:1430-1438.